3-D effects on viscosity and generation of toroidal and poloidal flows in LHD

K. Nagaoka, K. Ida, M. Yoshinuma, Y. Suzuki, K. Kamiya et al.

Citation: Phys. Plasmas **20**, 056116 (2013); doi: 10.1063/1.4807126
View online: http://dx.doi.org/10.1063/1.4807126
View Table of Contents: http://pop.aip.org/resource/1/PHPAEN/v20/i5
Published by the AIP Publishing LLC.

3-D effects on viscosity and generation of toroidal and poloidal flows in LHD[a)]

K. Nagaoka,[1,b)] K. Ida, M. Yoshinuma,[1] Y. Suzuki,[1] K. Kamiya,[2] S. Satake,[1] K. Tanaka,[1] M. Yokoyama,[1] S. Murakami,[3] M. Osakabe,[1] H. Takahashi,[1] R. Seki,[1] C. Suzuki,[1] Y. Narushima,[1] H. Nakano,[1] M. Kisaki,[1] K. Ikeda,[1] K. Tsumori,[1] Y. Takeiri,[1] O. Kaneko,[1] H. Yamada,[1] and LHD Experiment Group[1]
[1]*National Institute for Fusion Science, Toki 509-5292, Japan*
[2]*Japan Atomic Energy Agency, Naka, 311-0193, Japan*
[3]*Department of Nuclear Engineering, Kyoto University, Kyoto 615-8530, Japan*

(Received 16 November 2012; accepted 6 May 2013; published online 22 May 2013)

Three-dimensional effects on plasma flows have been experimentally studied in the large helical device with 3D configurations. Spontaneous toroidal flow without net driving force using the combination of perpendicular neutral beam injection (NBI) heating and balanced tangential NBI heating has been investigated with two magnetic configurations. Co- and counter-directed spontaneous flows have been observed depending on the collisionality. Toroidal flow shear changes the sign at $0.4 < r_{\mathrm{eff}} < 0.6$ between co- and counter-flowing plasmas, where r_{eff} is a averaged minor radius. The detailed flow structures have been also examined at the edge region with stochastic magnetic field. A poloidal flow driven by the positive radial electric field has been observed at the open field region just outside of the plasma boundary. At the stochastic region, a shear of poloidal flow has been observed, while no shear of toroidal flow has been observed. The toroidal flow shear changes only in the nested magnetic flux surface region. A difference of density fluctuation property has been observed between co- and counter-flowing plasmas, where toroidal flow shears are formed. © *2013 AIP Publishing LLC*. [http://dx.doi.org/10.1063/1.4807126]

I. INTRODUCTION

Spontaneous or intrinsic toroidal flows have been intensively studied and are considered to be important for reactor-scale tokamak plasmas,[1–4] because toroidal flow is needed to stabilize MHD instabilities and an external torque to drive plasma flow is not sufficient. A scaling law for spontaneous toroidal flow has been obtained for H-mode in tokamak plasmas and reported in Ref. 5. The spontaneous flow in L-mode plasmas shows non-linear properties such as the flow reversal,[6] and the correlation between the transition of the flow and the fluctuation properties has been discussed in Ref. 7.

Resonant magnetic perturbation (RMP) is recognized as a control knob of edge localized modes (ELMs)[8] and will be utilized in ITER. However, the toroidal flow is also affected by RMP field.[9] The reduction of toroidal flow was experimentally observed when an ELM activity is suppressed by RMP field.[10] Therefore, 3D effects on plasma flow is a key issue for reliable prediction of plasma flow in future devices with RMP field.

Plasma flows, both toroidal and poloidal, have also been studied in the helical plasmas, in which the magnetic configuration is intrinsically three-dimensional.[11–14] There is an effect of flow damping in helical plasmas even in the toroidal direction caused by non-axisymmetry in toroidal direction, which is called the "parallel viscosity" and has been experimentally confirmed in the compact helical system (CHS) for the first time.[11,15] Spontaneous flows driven by radial electric field and ion temperature gradient were also observed where the parallel viscosity is relatively large,[16,17] and they are qualitatively consistent with neoclassical prediction. Recently, a large offset toroidal flow was observed with ion internal transport barrier (ion ITB) formation in the large helical device (LHD) and correlates with ion temperature gradient.[13] The dynamic behavior of the toroidal flow was investigated with ion ITB formation, and a hysteresis curve was observed in the relation between velocity shear and ion temperature gradient.[18] These observations provide evidence of nonlinear bifurcation of spontaneous flow even in the 3D helical plasmas.

In this paper, spontaneous flows, which are observed without net external driving force, are discussed in the context of the 3D geometry of the helical plasma in LHD. The experimental setup is described in Sec. II, and the experimental results on the spontaneous toroidal flow are presented in Sec. III. Observations of poloidal flow driven by positive radial electric field at the edge region with stochastic magnetic field are also presented. Characteristics of density fluctuations of co- and counter-flowing plasmas are discussed in the region where the toroidal flow shears are formed. Finally, the results of these studies are summarized in Sec. IV.

II. EXPERIMENTAL SETUP

Experiments have been performed in the LHD, which is a device of the heliotron configuration with toroidal and poloidal periods of $l = 10$ and $m = 2$, respectively. The major and averaged minor radii are 3.9 and 0.6 m, respectively. A magnetic field up to 3 T is produced by super-conducting coils. Three tangential neutral beam injectors (NBIs) and two perpendicular (radial) NBIs have been installed. The

[a)]Paper NI3 4, Bull. Am. Phys. Soc. **57**, 203 (2012).
[b)]Invited speaker.

total port-through power is 16 MW for the tangential NBIs and 12 MW for the perpendicular NBIs.[19] In this experiment, the combination of perpendicular NBIs and balanced tangential NBIs have been used for plasma heating without net driving force of toroidal flow. The co-directed force is caused by the difference of particle orbit between co- and counter-injected beam ions and charge-exchange loss even in the balanced NBI, and is confirmed by FIT-3D code[20] to be negligibly small in this experimental condition with high magnetic field. The co-direction refers to the toroidal current direction that increases the rotational transform (inverse safety factor: $1/q$).

A charge exchange spectroscopy (CXS) system has been installed on LHD to measure profiles of ion temperature, toroidal and poloidal flows, and carbon density.[21] A large number of chords are installed with tangential and radial lines of sight and observe the emission line from the charge exchange recombination of fully ionized carbon (Carbon VI: $\lambda = 529.05$ nm). The fast CXS system (with a time resolution up to 400 Hz and 53 channels) and slow CXS system (with a time resolution of 20 Hz and 79 channels) are operated simultaneously. The spatial resolution (spot size) of each chord is 2 cm for both CXS systems. The perpendicular NBI (BL-4) with the beam energy of 40 kV is used as a probe beam with beam modulation technique to allow subtraction of the background signal.

III. EXPERIMENTAL RESULTS

The toroidal plasma flows observed in LHD are mainly determined by four elements; external driving force due to tangential NBIs, perpendicular momentum transport (viscosity), parallel viscosity (neoclassical viscosity), and turbulence driven spontaneous flow (residual stress). The radial diffusion of toroidal flow (momentum) is well correlated with ion heat diffusivity and of the same order of magnitude.[13,22] The parallel viscosity is a damping effect of the parallel flow with respect to the magnetic field lines due to 3D effects and can be controlled by the position of the magnetic axis. The toroidal flow driven by external force or torque (tangential NBI) is affected by the parallel viscosity and decreases with outward shifted plasmas, where the parallel viscosity becomes large. In this study, spontaneous toroidal flows without net external driving force have been investigated in two magnetic field configurations with relatively weak parallel viscosity ($R_{ax} = 3.60$ m and $R_{ax} = 3.75$ m). The effective helical ripple, ϵ_{eff},[23] of the configuration of $R_{ax} = 3.60$ m is almost one third of that of the configuration of $R_{ax} = 3.75$ m. Here, ϵ_{eff} is one of measure for the non-axisymmetry of magnetic configuration in helical systems.

A. Spontaneous toroidal flow with 3D geometry

The counter-directed toroidal flow was observed in the plasma heated by perpendicular NBI with port through power of $P_{port} = 4.4$ MW, which is shown in Fig. 1. The neoclassical transport was calculated with the FORTEC-3D code,[24] and the radial electric field (E_r) and the poloidal flow including diamagnetic drift well agrees with experimental observations (Figs. 1(b) and 1(c)). However, a discrepancy is observed in toroidal flow (Fig. 1(d)). The measurement of toroidal flow by the CXS diagnostic has an uncertainty in

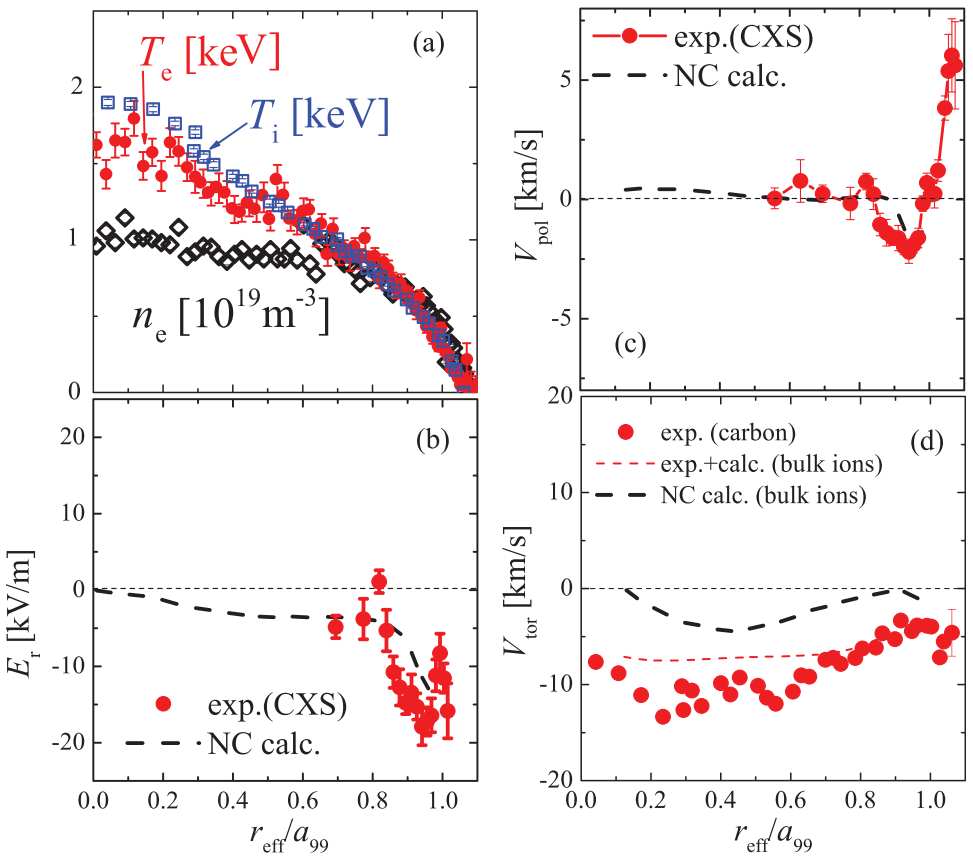

FIG. 1. (a) The profiles of electron temperature, ion temperature, and electron density as a function of normalized minor radius, where r_{eff} and a_{99}(= 0.625) are the averaged minor radius and plasma size, which encompasses 99% of the electron stored energy, respectively. Profiles are shown of (b) the radial electric field, (c) the poloidal flow, and (d) the toroidal flow. The predictions of neoclassical theory calculated by FORTEC-3D code are plotted by dashed lines in (b), (c), and (d). The toroidal flow measurement with the CXS diagnostic have an uncertainty ($\delta V_{tor} = 4.5$ km/s) in the absolute value, which is shown in (d). The poloidal flow can be measured with much higher accuracy than toroidal flow. In a strict sense, this is a velocity of carbon impurity flow, and the bulk hydrogen ions have a slightly different flow velocity. The difference of flow velocity between carbon and hydrogen ions was evaluated by neoclassical code GSRAKE,[25] and the calibrated flow velocity of bulk hydrogen ions is also shown by dashed red lines.

absolute value due to the difficulty of calibration. The flow velocity difference (δV) also exists between carbon impurity and bulk ions (hydrogen), and it can be calculated by neoclassical theory. The closed circles in red in Fig. 1(d) show the velocity of carbon impurity measured by CXS, and the dashed line in red shows the bulk ion velocity, which is evaluated by the measured carbon impurity velocity and the calculated flow velocity difference (δV) with the GSRAKE code.[25] Moreover, the calculated toroidal flow profile with the FORTEC-3D code is an averaged profile on the magnetic flux surface in a Boozer coordinate. Therefore, the detailed comparison of the local flow velocity in real coordinate is necessary for more quantitative discussion. The drift direction of precession motion of trapped particles is in the co-direction in LHD. Therefore, the observed counter-directed toroidal flow is considered as a spontaneous flow.

B. Collisionality dependence of spontaneous flow

The systematic parameter survey of spontaneous flow was carried out, and the heating power of NBI and the electron density were scanned in wide ranges from 2 MW to beyond 12 MW and from $0.5 \times 10^{19}\,\mathrm{m}^{-3}$ to $6 \times 10^{19}\,\mathrm{m}^{-3}$, respectively. The perpendicular NBI heating is utilized for all discharges, and balanced tangential NBI is also utilized for the scan of heating power. The net external driving force from NBI is small, amounting to only a few % of the driving force from each individual tangential NBI. Figure 2 shows summary of the toroidal flow observed at the normalized minor radius of $r_{\mathrm{eff}}/a_{99} = 0.6$. The co-directed spontaneous flow is also observed in low density region with both magnetic configurations.

The density gradient is recently considered to be important to characterize turbulent driven spontaneous flows.[26] Figure 2(b) shows the dependence of toroidal flow on the density gradient. In the case of $R_{\mathrm{ax}} = 3.60\,\mathrm{m}$, the density gradient is almost zero ($R/L_{\mathrm{n}} \sim 0$) for co- and counter-flowing plasmas. In the case of $R_{\mathrm{ax}} = 3.75\,\mathrm{m}$, the scale length of density gradients distribute around zero and negative region (hollow profile) when the strong gas puff is applied. There is no clear correlation between the spontaneous flow direction and density gradient in this experiment, which is similar to the spontaneous toroidal flow reversal observed in TCV tokamak.[6]

There found to exist two regions in the normalized collisionality as seen in Fig. 2(c). Here, the normalized collisionality, ν^*_{hi}, is defined by $\nu_{\mathrm{i}}/[\epsilon_{\mathrm{eff}}^{3/2}(V_{\mathrm{th}}/qR)]$. The spontaneous flow is co-direction in the low collisionality region and is counter-direction in high collisionality region. The collisionality is considered to be very important as a separation parameter of the direction of spontaneous toroidal flow, although it is not concluded from the limited data set whether the collisionality is the relevant parameter or not. A large discontinuity of spontaneous toroidal flow appears between co- and counter-directed flows. It is noted that this change of flow direction depending on collisionality is interesting from view point of the similarity to the toroidal flow reversal observed in tokamak plasmas with density ramp up operation.

The collisionality dependence of the spontaneous flow is different between the two magnetic field configurations, while the discontinuous change of toroidal flow exists in both configurations. In the case of outward shifted configuration of $R_{\mathrm{ax}} = 3.75\,\mathrm{m}$, the co-directed spontaneous flow decreases with collisionality, and counter-directed one in higher collisionality region also decreases with collisionality. On the other hand, in the case of inward shifted configurations of $R_{\mathrm{ax}} = 3.60\,\mathrm{m}$, the counter-directed flow slightly increases with collisionality, and no clear collisionality dependence of co-directed flow is observed. It is noted that the study of these difference of spontaneous flow between the different configurations is a direct approach to understand the 3D effects on toroidal flow generation.

C. Profile of spontaneous toroidal flows

In order to identify the difference between co- and counter-directed spontaneous flows, the profiles of spontaneous flow velocity are compared. Figure 3 shows the co- and counter-directed toroidal flow profiles with collisionality close to the separation point ($\nu^*_{\mathrm{hi}} = 20.3$ and $\nu^*_{\mathrm{hi}} = 31.0$, respectively). In this experiment, spontaneous flow was investigated in a wide range of plasma parameters such as density, heating power and so on, and these data were

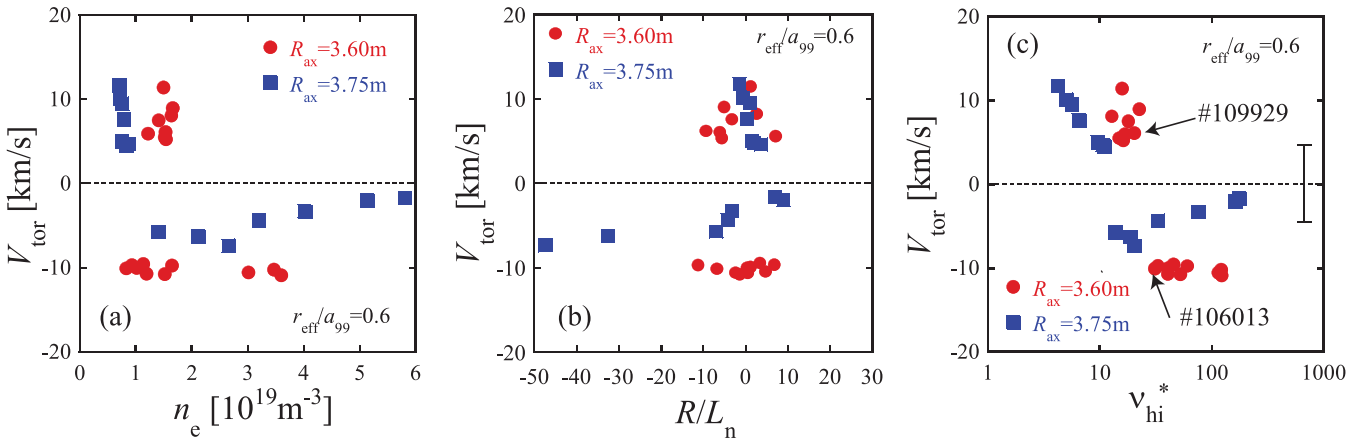

FIG. 2. Spontaneous flow velocity measured at $r_{\mathrm{eff}}/a_{99} = 0.6$ without net external driving force as functions of (a) electron density at $r_{\mathrm{eff}}/a_{99} = 0.6$, (b) normalized density gradient, and (c) the normalized collisionality.

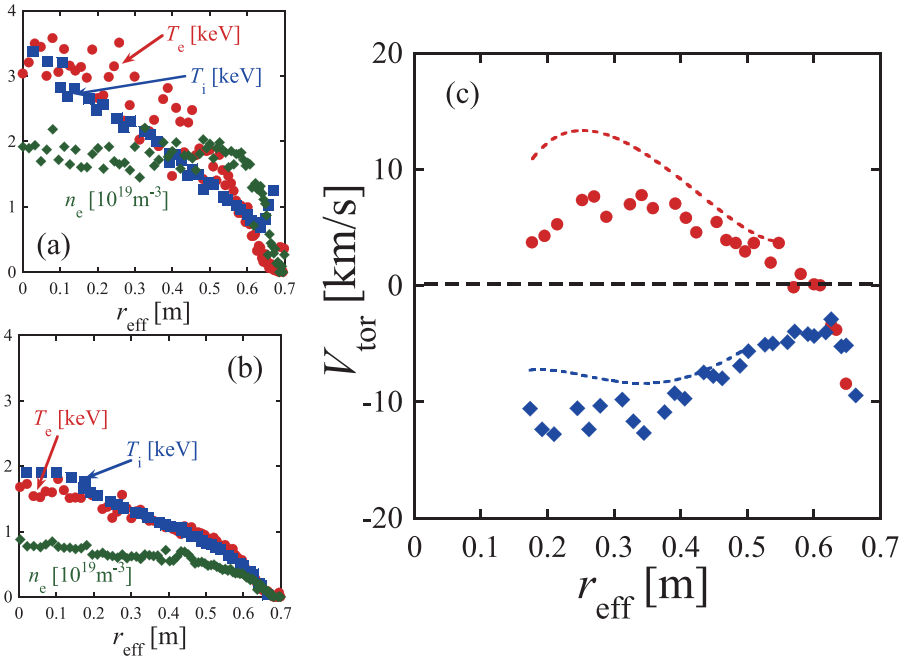

FIG. 3. The profiles of electron temperature, ion temperature, and electron density of (a) co-flowing plasma (SN. 109929, $R_{ax} = 3.60$ m, $\nu^*_{hi} = 20.3$) and (b) counter-flowing plasma (SN. 106013, $R_{ax} = 3.60$ m, $\nu^*_{hi} = 31.0$). These plasmas have collisionality close to the separation point. (c) The profiles of flow velocity in these plasmas are shown with closed circles. The flow velocity of bulk hydrogen ions calibrated with neoclassical theory is also shown by dashed lines.

obtained with shot by shot basis. The comparison of these two plasmas shown in Fig. 3 is considered to be useful to discuss the mechanism of flow generation contributing the observed flow reversal.

The co-flowing plasma shown in Fig. 3(a) is heated by balanced tangential NBIs (3.0 MW for co-NBI and 2.9 MW for counter-NBI) and perpendicular NBI (2.4 MW), and the density profile is flat. In this experiment, the power of tangential NBIs is well controlled and the unbalanced beam power is almost 0.1 MW. The orbit asymmetry between co- and counter-directed fast ions may cause unbalanced torque, and it is a few % of total input torque. The toroidal flow driven by the total unbalanced torque is evaluated as about 2 km/s, which is less than the error bar in flow measurement. On the other hand, the counter-flowing plasma shown in Fig. 3(b) is heated by only perpendicular NBI (3.4 MW), and the density profile is slightly peaked. The opposite sign of velocity shear was observed at $0.4 < r_{eff} < 0.6$ between co- and counter-flowing plasmas, which is shown in Fig. 3(c). From view point of flow generation, the observed flow shears are considered to overcome the viscous damping to sustain the toroidal flow in the core region.

D. Flow structure at the edge region with stochastic magnetic field

The edge region in 3D systems is very complicated because the magnetic field lines become stochastic and the plasma boundary become unclear. Here, the flow structures of spontaneously flowing plasmas shown in Fig. 3 are discussed in the three regions; the nested flux surface region, stochastic region in the confined plasma, and the open field region outside of the plasma boundary. The plasma boundary is determined by the maximum E_r shear position. This method to determine the plasma boundary has been proposed with physical basis whether the plasma is directly affected by the wall or not.[28] The boundary determined by the maximum E_r shear has been compared with numerical modeling and is almost identical to the position where the connection length of the magnetic field become short with respect to the electron mean-free-path.[29]

The poloidal and toroidal flow profiles of co- and counter-flowing plasmas near the edge region are shown in Figs. 4(a) and 4(b), respectively. The Poincaré maps of the magnetic field of each plasma are also shown in Figs. 4(c) and 4(d), respectively. The stochastic region (hatching region in the Fig. 4) and the plasma boundary position of both plasmas are almost identical. The poloidal flow structures are similar to each other, though a slight difference is observed in the nested flux surface region. The poloidal flows have a peak at the open field region just outside of plasma boundary. The localized poloidal flow is driven by a positive radial electric field, which is produced by the parallel transport of electrons to the wall. The poloidal flow shear is observed in the stochastic region and the nested flux surface region, while the flow shear becomes weak in the nested flux surface region.

The toroidal flows in the stochastic region seem to be almost the same between co- and counter-flowing plasmas, and no clear flow shear was observed in this region. In the open field region outside of the plasma boundary, flow in the counter-direction has been observed in both plasmas. These counter-flows with positive radial electric field seem to be consistent with the observations of radial electric field driven flow in the nested flux surface region in CHS[30] and LHD,[17] although the effects of the stochastic magnetic field should be taken into account. The opposite sign of toroidal flow shear between two plasmas shown in Fig. 4 is observed in the nested flux surface region, not in the stochastic magnetic field region.

E. Observation of density fluctuation

Here we discuss on the change of spontaneous toroidal flow direction in the core region, which is caused by the

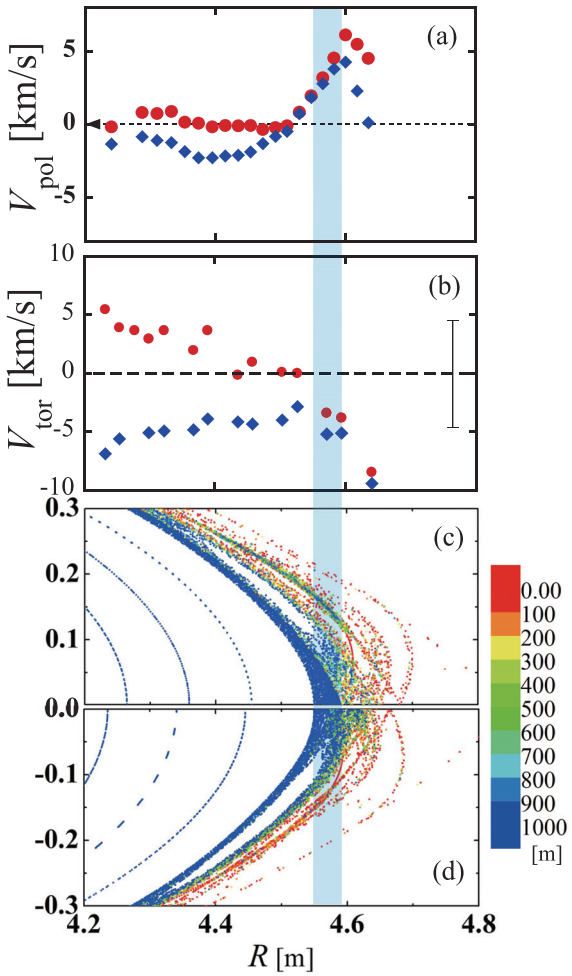

FIG. 4. (a) The poloidal flow velocity and (b) the toroidal flow velocity profiles. (c) Poincaré map of the magnetic field at the horizontally elongated cross section of the co-flowing and (d) counter-flowing plasmas shown in Figs. 3(a) and 3(b), respectively.

change of sign of flow shear at $0.4 < r_{\rm eff} < 0.6$. Neoclassical viscosity has a possibility to cause the change of spontaneous flow direction due to a bifurcation of radial electric field. However, no bifurcation of radial electric field was observed between co- and counter-flowing plasmas in this experiment. Another candidate is a turbulent driven component of spontaneous flow, because residual stress may change the sign depending on turbulence property.[31,32] Other effects such as ion orbit loss effect are not considered to cause a discontinuous change of flow direction, although they may contribute the absolute value of toroidal flow velocity. Therefore we focus on the fluctuation property in the region of $0.4 < r_{\rm eff} < 0.6$.

Two-dimensional phase contrast imaging (2D-PCI) diagnostic was used for measurement of density fluctuation property in this experiment.[27] The 2D-PCI in LHD can measure the local density fluctuation and their propagating velocity perpendicular to the magnetic field (poloidal dominated). Figure 5 shows the fluctuation as a function of averaged minor radius and propagation velocity for (a) co- and (b) counter-flowing plasmas, which are the same plasmas shown in Figs. 3(a) and 3(b), respectively. The 2D-PCI data shown in Fig. 5 are time-averaged for 0.1 s with the frequency range of 20–500 kHz and with the wavelength of $k = 0.1$–$1\ \mathrm{mm}^{-1}$.

As shown in Fig. 5, a drastic change of density fluctuation characteristics is observed. In the co-flowing case, the largest peak of density fluctuation is located at $r_{\rm eff} = 0.4$ m and propagates toward the ion diamagnetic direction in laboratory frame, and another peak at $r_{\rm eff} = 0.58$ m propagates toward the electron diamagnetic direction. On the other hand, in the counter flowing case, a single peak of density fluctuation is visible at $r_{\rm eff} = 0.48$ m and propagates toward electron-diamagnetic direction in laboratory frame. The propagation direction in the plasma frame should be discussed to investigate the fluctuation properties and their contribution to the flow drive. The $E \times B$ drift velocity, estimated by radial electric field, was plotted by a blue line in Fig. 5. The propagation direction of the observed fluctuation in the counter-flowing plasma in the plasma frame is unclear, while the largest fluctuation in the co-flowing plasma propagates in the ion-diamagnetic direction in the plasma frame. It should be noted that in the co-flowing plasma, the mode propagating in the electron diamagnetic direction in the plasma frame is observed near the edge where the change of spontaneous flow direction depending on collisionality was observed, and such mode does not appear in the counter-flowing plasma. It is interesting that a similar phenomenon was observed in Alcator C-mod tokamak plasma, when toroidal flow reverses spontaneously.[7] It is also noted that a change of radial electric field shear is

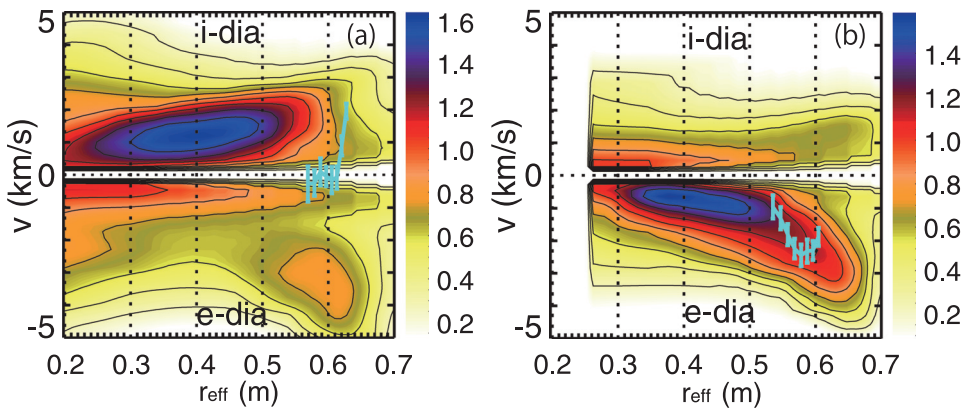

FIG. 5. Density fluctuation measured by a 2D-PCI diagnostic of (a) co-flowing plasma and (b) counter-flowing plasma, which are the same plasma shown in Figs. 3(a) and 3(b), respectively. Color indicates the amplitude in a logarithmic scale ($\log \tilde{n}_e$ (arb. units)). The vertical axis denotes propagating velocity perpendicular to the magnetic field (poloidal dominated). The positive velocity is in the ion-diamagnetic drift direction. The $E \times B$ drift velocity is also shown with blue lines.

observed near the edge region between co- and counter-flowing plasmas. Further investigation is necessary to identify the physics mechanism of generation of spontaneous torque near the edge, which can explain the change of toroidal flow direction observed in LHD.

IV. SUMMARY

Plasma flow without net external driving force has been investigated in a 3D system. The spontaneous toroidal flow was driven in the both co- and counter-directions with flat density profile. A discontinuous change of toroidal flow was observed between co- and counter-flowing plasmas depending on collisionality. A poloidal flow is driven at the open field region where positive E_r is produced by parallel transport of electrons to the wall. A poloidal flow shear is observed at the stochastic region in the confined plasma, while no clear difference is observed in toroidal flow between co- and counter-flowing plasmas. A change of toroidal flow shear is observed in the nested flux surface region ($0.4 < r_{eff} < 0.6$). The density fluctuation in the edge region of co-flowing plasma is not observed in counter-flowing plasma. A different radial electric shear near the edge region is observed between co- and counter-flowing plasmas, where the change of toroidal flow direction is observed depending on the collisionality. It is very important subject to identify the physics mechanism of spontaneous torque generation at the edge region in LHD, where parallel viscosity is significant. The studies of spontaneous toroidal flow in LHD suggest that the flow generation with 3D geometry as well as flow damping (neoclassical toroidal viscosity) should be studied in the peripheral region of tokamak plasmas when RMP field is applied. Study of configuration dependence of spontaneous flow in LHD and comparison of the spontaneous flow mechanism between tokamak and helical plasma are necessary for further understanding of 3D effects on spontaneous flow drive, which is left for future studies.

ACKNOWLEDGMENTS

The authors thank Professor K. Itoh and Professor A. Komori (National Institute for Fusion Science) for their fruitful discussions and encouragements, and also thank Professor J. E. Rice (Massachusetts Institute of Technology) and T. E. Evans (General Atomics) for their fruitful discussions. The authors also thank Dr. N. A. Pablant (Princeton Plasma Physics Laboratory) for his help of English correction of our manuscript. The authors also thank LHD staff for their excellent operation of LHD experiments. This work was supported by LHD12ULRR702.

[1]P. H. Diamond, C. J. McDevitt, Ö. D. Gürcan, T. S. Hahm, W. X. Wang *et al.*, Nucl. Fusion **49**, 045002 (2009).
[2]K. Ida, Y. Miura, K. Itoh, S. Hidekuma, S.-I. Itoh *et al.*, Phys. Rev. Lett. **74**, 1990 (1995).
[3]K. Ida, Y. Miura, K. Itoh, S.-I. Itoh, and T. Matsuda, J. Phys. Soc. Jpn. **67**, 4089 (1998).
[4]J. E. Rice, P. T. Bonoli, J. A. Goetz, M. J. Greenwald, I. H. Hutchinson *et al.*, Nucl. Fusion **39**, 1175 (1999).
[5]J. E. Rice, A. Ince-Cushman, J. S. deGrassie, L.-G. Eriksson, Y. Sakamoto *et al.*, Nucl. Fusion **47**, 1618 (2007).
[6]A. Bortolon, B. P. Duval, A. Pochelon, and A. Scarabosio, Phys. Rev. Lett. **97**, 235003 (2006).
[7]J. E. Rice, B. P. Duval, M. L. Reinke, Y. A. Podpaly, A. Bortolon *et al.*, Nucl. Fusion **51**, 083005 (2011).
[8]Y. Liang, H. R. Koslowski, P. R. Thomas, E. Nardon, and B. Alper, Phys. Rev. Lett. **98**, 265004 (2007).
[9]K. H. Finken, S. S. Abdullaev, M. F. M. de Bock, M. von Hellermann *et al.*, Phys. Rev. Lett. **94**, 015003 (2005).
[10]T. E. Evans, R. A. Moyer, P. R. Thomas, J. G. Watkins *et al.*, Phys. Rev. Lett. **92**, 235003 (2004).
[11]K. Ida and N. Nakajima, Phys. Plasmas **4**, 310 (1997).
[12]M. Yoshinuma, K. Ida, M. Yokoyama, K. Nagaoka, M. Osakabe *et al.*, Plasma Fusion Res. **3**, S1014 (2008).
[13]K. Nagaoka, K. Ida, M. Yoshinuma, Y. Takeiri, M. Yokoyama *et al.*, Nucl. Fusion **51**, 083022 (2011).
[14]A. Briesemeister, K. Zhai, D. T. Anderson, F. S. B. Anderson, J. Lore, and J. N. Talmadge, Contrib. Plasma Phys. **50**, 741 (2010).
[15]K. Ida, H. Yamada, H. Iguchi, K. Itoh *et al.*, Phys. Rev. Lett. **67**, 58 (1991).
[16]K. Ida, T. Minami, Y. Yoshimura, A. Fujisawa, C. Suzuki *et al.*, Plasma Phys. Controlled Fusion **44**, 361 (2002).
[17]M. Yoshinuma, K. Ida, M. Yokoyama, K. Nagaoka, M. Osakabe *et al.*, Nucl. Fusion **49**, 075036 (2009).
[18]K. Ida, M. Yoshinuma, K. Nagaoka, M. Osakabe, S. Morita *et al.*, Nucl. Fusion **50**, 064007 (2010).
[19]Y. Takeiri, O. Kaneko, K. Tsumori, M. Osakabe, K. Ikeda, K. Nagaoka *et al.*, Fusion Sci. Technol. **58**, 482 (2010).
[20]S. Murakami, N. Nakajima, and M. Okamoto, Fusion Technol. **27** (Suppl. S), 256 (1995).
[21]K. Ida, S. Kado, and Y. Liang, Rev. Sci. Instrum. **71**, 2360 (2000).
[22]H. Takahashi, M. Osakabe, K. Nagaoka, S. Murakami *et al.*, in *23th International Conference on Fusion Energy, San Diego, 2012* (International Atomic Energy Agency, Vienna, 2013), EX/2-5.
[23]C. D. Beidler and W. N. G. Hitchon, Plasma Phys. Controlled Fusion **36**, 317 (1994).
[24]S. Satake *et al.*, Plasma Phys. Controlled Fusion **53**, 054018 (2011).
[25]C. D. Beidler and W. D. D'haeseleer, Plasma Phys. Controlled Fusion **37**, 463 (1995).
[26]C. Angioni, R. M. McDermott, F. J. Casson, E. Fable *et al.*, Phys. Rev. Lett. **107**, 215003 (2011).
[27]K. Tanaka, C. A. Michael, L. N. Vyacheslavov, A. L. Sanin, K. Kawahata *et al.*, Rev. Sci. Instrum. **79**, 10E702 (2008).
[28]K. Kamiya, K. Ida, M. Yoshinuma, C. Suzuki, Y. Suzuki, M. Yokoyama *et al.*, Nucl. Fusion **53**, 013003 (2013).
[29]Y. Suzuki, K. Ida, S. Sakakibara, M. Yoshinuma, K. Y. Watanabe *et al.*, *23th International Conference on Fusion Energy, San Diego, 2012* (International Atomic Energy Agency, Vienna, 2013), EX/8-2.
[30]K. Ida, T. Minami, Y. Yoshimura, A. Fujisawa, C. Suzuki *et al.*, Phys. Rev. Lett. **86**, 3040 (2001).
[31]Ö. D. Gürcan, P. H. Diamond, T. S. Hahm, and R. Shingh, Phys. Plasmas **14**, 042306 (2007).
[32]W. M. Solomon, K. H. Burrell, J. S. deGrassie, J. A. Boedo *et al.*, Nucl. Fusion **51**, 073010 (2011).